Scholars' Mine

Masters Theses   Student Theses and Dissertations

1971

Evaporation and condensation of zinc

Shailesh Bhanuprasad Vora

Follow this and additional works at: https://scholarsmine.mst.edu/masters_theses

Part of the Metallurgy Commons

Department:

Recommended Citation

EVAPORATION AND CONDENSATION OF ZINC

BY

SHAILESH BHANUPRASAD VORA, 1945

A Thesis

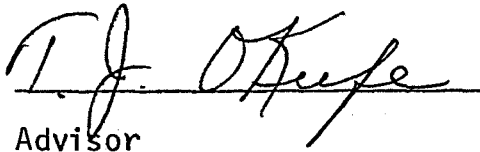Presented to the Faculty of the Graduate School of the

UNIVERSITY OF MISSOURI - ROLLA

In Partial Fulfillment of the Requirements for the Degree
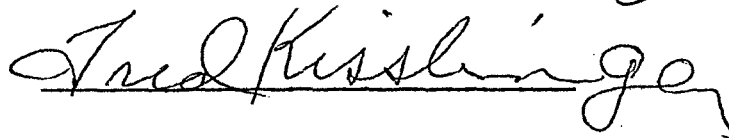
MASTER OF SCIENCE IN METALLURGICAL ENGINEERING

1971

Approved by

_____ _____
Advisor

_____

PUBLICATION THESIS OPTION

This thesis has been prepared in the style utilized by the
Transactions of the Metallurgical Society of AIME. Pages 1-30 will
be presented for publication in that journal. Appendices A,B, and
C have been added for purposes normal to thesis writing.

ABSTRACT

Evaporation rates of liquid zinc were determined experimentally within the temperature range of 450° C to 575° C and at argon pressures ranging from 730mm Hg to 130mm Hg. Extrapolated values of these rates are found to be consistent with the previously reported rates obtained by St. Clair and Spendlove at lower pressures. Between 100 microns and one atmosphere pressure, rates of evaporation seem to vary according to an equation of the form $W = AP^B$, where P is pressure and, A and B are constants. Similar experiments were performed with brass powders in atmospheres of argon and helium at temperatures between 550° C and 650° C. The kinetics of sublimation of zinc from brass powders were found to be consistent with the evaporation behavior from a liquid zinc bath. The effect of various process conditions on the morphology of zinc condensed from the vapor phase was also determined.

ACKNOWLEDGEMENTS

TABLE OF CONTENTS

LIST OF FIGURES

INTRODUCTION

A need exists to determine and predict practically obtainable rates of evaporation of zinc and other non-ferrous metals, particularly at one atmosphere and lower pressures. Such information could be very useful since it is becoming increasingly important to improve on the efficiency of recovery of metal values from secondary source materials and the comparatively high vapor pressure of zinc makes the selective evaporation more attractive. One of the earliest evaporation studies on liquid zinc was carried out by St. Clair and Spendlove.[1,2] In their experiments, pressures of 10 to 5000 microns were used. Their data do not give detailed rate-pressure relationship but do indicate that the rate decreases proportionally with increasing pressure and decreasing power supplied to the induction furnace. The scatter of the data in those reports was very high due to the nature of the experimental procedure. In the present investigation, working pressures from one atmosphere to 100 mm Hg were selected to determine the nature of the evaporation process in which mass transport through a residual gas is important since most previous work has been conducted in a commercial vacuum range or lower.

Similar experiments were also conducted on brass powders to determine the evaporation behavior of zinc when present in some state other than unit activity. A typical composition of 70 Cu : 30 Zn was chosen. Wu[3] has shown that the rates of evaporation of zinc are higher in helium than in argon. Hence, experiments on brass were conducted using both of these gases.

Metal vapors can be successfully utilized to form powders and different uses of zinc powders dictate the need for a variety of particle sizes and shapes. Wada[4] has shown that the size of particles increases with increases in pressure in the range of 5 to 350 torr. Butler[5] has described a newly developed system of vacuum vapor deposition of zinc on a continuous steel-strip substrate, at a pressure of about 2×10^{-4} torr. A series of experiments was carried out in the present work to determine the possibility of forming various morphologies and orientations of zinc powders and deposits.

EXPERIMENTAL

All the experiments for determination of the rates of evaporation of zinc and brass were conducted on a Mettler Instrument Corporation Thermoanalyzer. The unit consists of four main parts: balance housing, recorder, furnace, and crucible support.

The balance is designed on a substitution principle. The built-in set of switch weights and electric tare compensation allow a maximum load of 16 gm. when weighed above the balance mechanism. The incorporation of a rotary pump and two diffusion pumps within the balance housing provide easy control of pressure in the sample compartment. A twelve point recorder provides a simultaneous indication of weight and temperature. The temperature controller can be programmed to give a heating or cooling rate of 0.5, 1.0, 1.5, 2, 4, 6, 8, and 10 $^\circ$c/min. For the present investigation, a rate of 10 $^\circ$c/min. was selected for all the experiments. On the weight scale, 10 mg. full scale range on the recorder was chosen. The furnace, which surrounds the sample, consists of a bifilar quartz tube system which is sealed at the upper end. The crucible support which fits into the socket which is connected to the arm of the balance, consists of a thin alumina tube which contains a Pt Rh 10%-Pt thermocouple whose hot junction touches the base of the crucible when the latter is positioned on the support. A photograph of the arrangement is shown in fig. 20 with the furnace placed behind the crucible and the support for clarity. During an actual experiment, the furnace encloses both the crucible and the support.

The alumina crucibles supplied for use with this unit were

found to be too small and fragile for efficient use. Hence, special crucibles, one of which is shown in fig. 20 on the crucible support, were made by attaching a 2 cm. long piece of alumina tubing (coors/ AD-99, 0.125" ID) to the bottom of a 22 mm OD cylindrical alumina crucible (coors/AD-998,CN6) and joining them with high temperature ceramic adhesive (Ultra-Temp 516 made by Aremco Products, Inc.).

Zinc slab of 99.99% purity was pre-cast into rods of approximately the same diameter as that of crucible. Small (7 to 8 gm.) slices were cut from it and used as samples. These samples were carefully cleaned by filing and then washed in acetone. The crucible support was placed in the socket and the crucible with the clean sample in it was placed on the support before the furnaced was positioned. The furnace was evacuated and back filled with argon which had been passed over getter chips (87.5% Zr, 12.5% Ti; Oregon Metallurgical Corp.) heated to 900° C. The procedure of evacuation and refilling was repeated three times to ensure as complete a removal of oxygen and moisture from the system as practically feasible. The sample was then weighed and the scale indication of the weight was brought to a convenient location on the recorder. A 5 to 6 ^{cc}/min flow rate of gas was maintained for all evaporation experiments conducted at one atmosphere. To attain pressures lower than one atmosphere, the balance was momentarily arrested and the pressure was adjusted to the desired value by partial evacuation using the vacuum pump. Due to the nature of the equipment, the temperature could be changed during the experiment. The rate of weight loss was determined from the slope of the weight curve on a 10 mg. full scale at a constant temperature and pressure. The procedure used for the sublimation
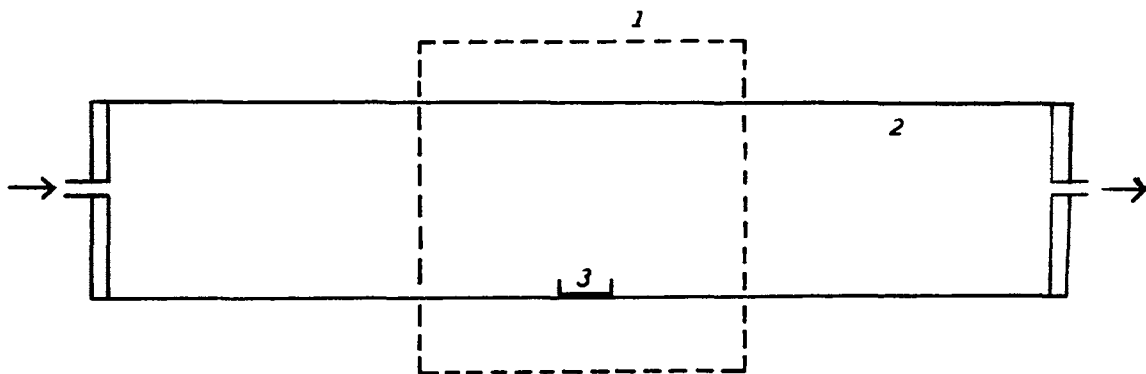
1. FURNACE   2. VYCOR TUBE   3. CRUCIBLE

CONDENSATION OF ZINC

Fig. 1

rate of zinc from brass was similar to that used for pure zinc. It should be noted that the rate of weight loss in the case of brass powders was calculated on the basis of projected cross-sectional area of the crucible and not on the actual surface area of brass particles. Two different samples of brass were used; Brass I (70% Cu, 30% Zn) from New Jersey Zinc Co., manufactured about 20 years ago and Brass II (73% Cu, 27% Zn), a recent sample from United Bronze Powders, Inc.

To study the condensation of zinc, the pure metal was evaporated from an alumina crucible placed in a 80 cm. long, 25 mmId, horizontal vycor tube, as shown in fig. 1. The tube was evacuated, back filled with gas, argon or helium, and placed in the furnace which had been heated to the desired temperature. The condensation was carried out at various pressures. At higher pressures, from one atmoshpere to about 200 mm Hg, the condensate was collected in powder form. These were examined using a scanning electron microscope. At low pressures (below 10-20 mm Hg), the metal was observed to deposit as a continuous film on the inside surface of the tube. This film was then scraped and also examined using SEM.

RESULTS

The observed rates of evaporation of liquid zinc at different temperatures and pressures are given in Appendix B. Of the large number of experiments made on liquid zinc, these values correspond to one particular run where the surface of the sample appeared to be brightest. However, these values are reproducible whenever the sample surface is bright and oxide free. The rates were observed to decrease when there was an oxide layer covering the liquid surface, with the decrease usually being directly proportional to the amount of oxide present. Fig. 2 shows Arrhenius type plot of the rates.

The maximum rate of evaporation from a liquid surface, given by kinetic theory[6], is

$$W_{max.} = Po \left(\frac{M}{2\pi RT}\right)^{\frac{1}{2}}$$

where $W_{max.}$ is the rate of evaporation in $gm/_{cm}{}^2.min.$, Po is the vapor pressure of the liquid in $dynes/_{cm}{}^2$ at temperature $T^{\circ}K$, M is the molecular weight of the liquid and R is the gas constant in $ergs/mole \ ^{\circ}K$. The vaporization coefficient is neglected here because it has been reported to be approximately one, particularly for liquids. The above equation can be simplified for zinc evaporation as:

$$W_{max} = W_{vac.} = \frac{28.3 \ Po}{T^{\frac{1}{2}}}$$

where $W_{max.}$ and T are defined above, and Po is the vapor pressure of zinc in mm Hg. These rates can be realized only in a perfect vacuum, where every atom that leaves the surface of the liquid is

EVAPORATION OF ZINC IN ARGON
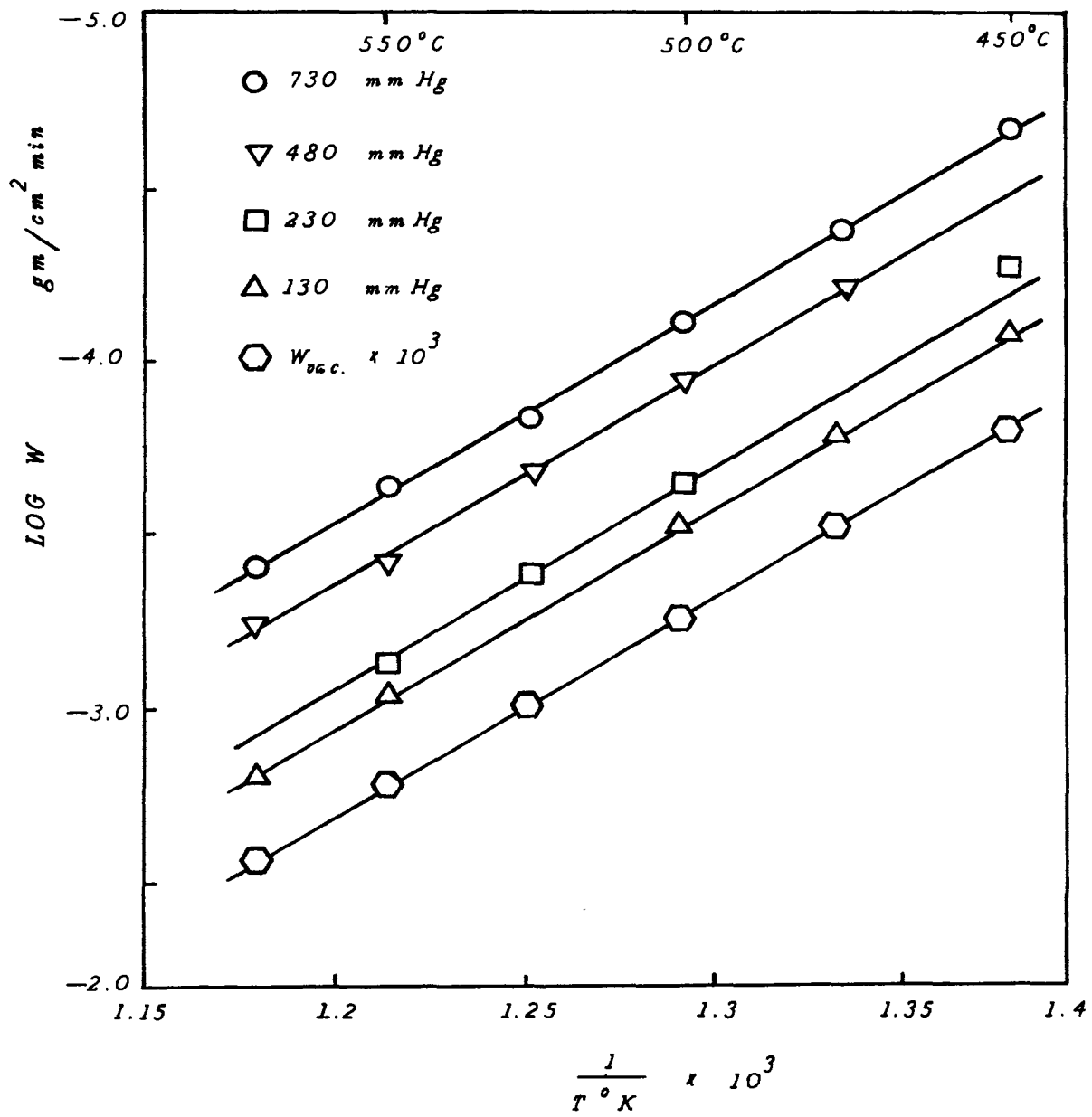
Fig. 2

EVAPORATION OF ZINC IN ARGON
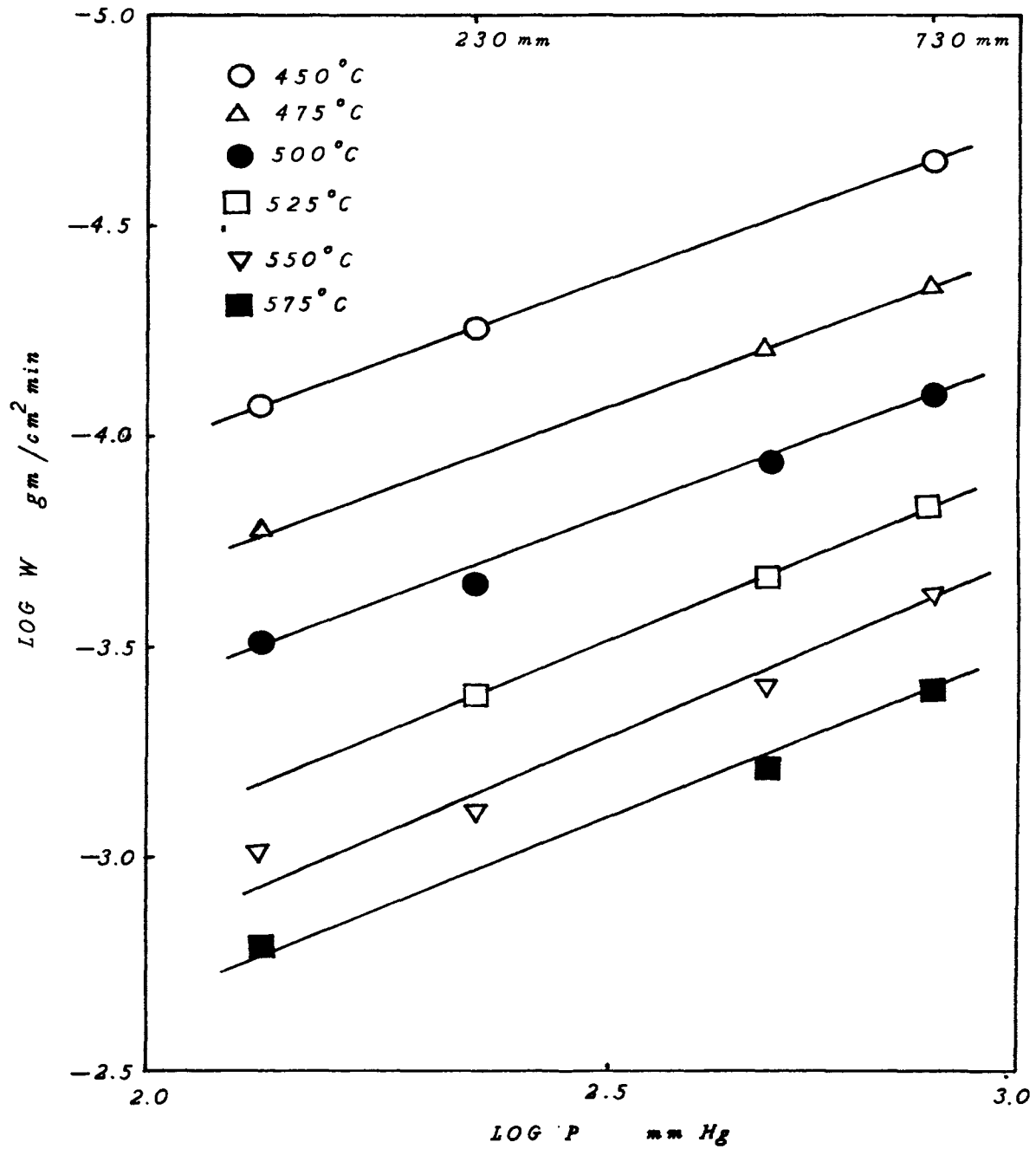
Fig. 3
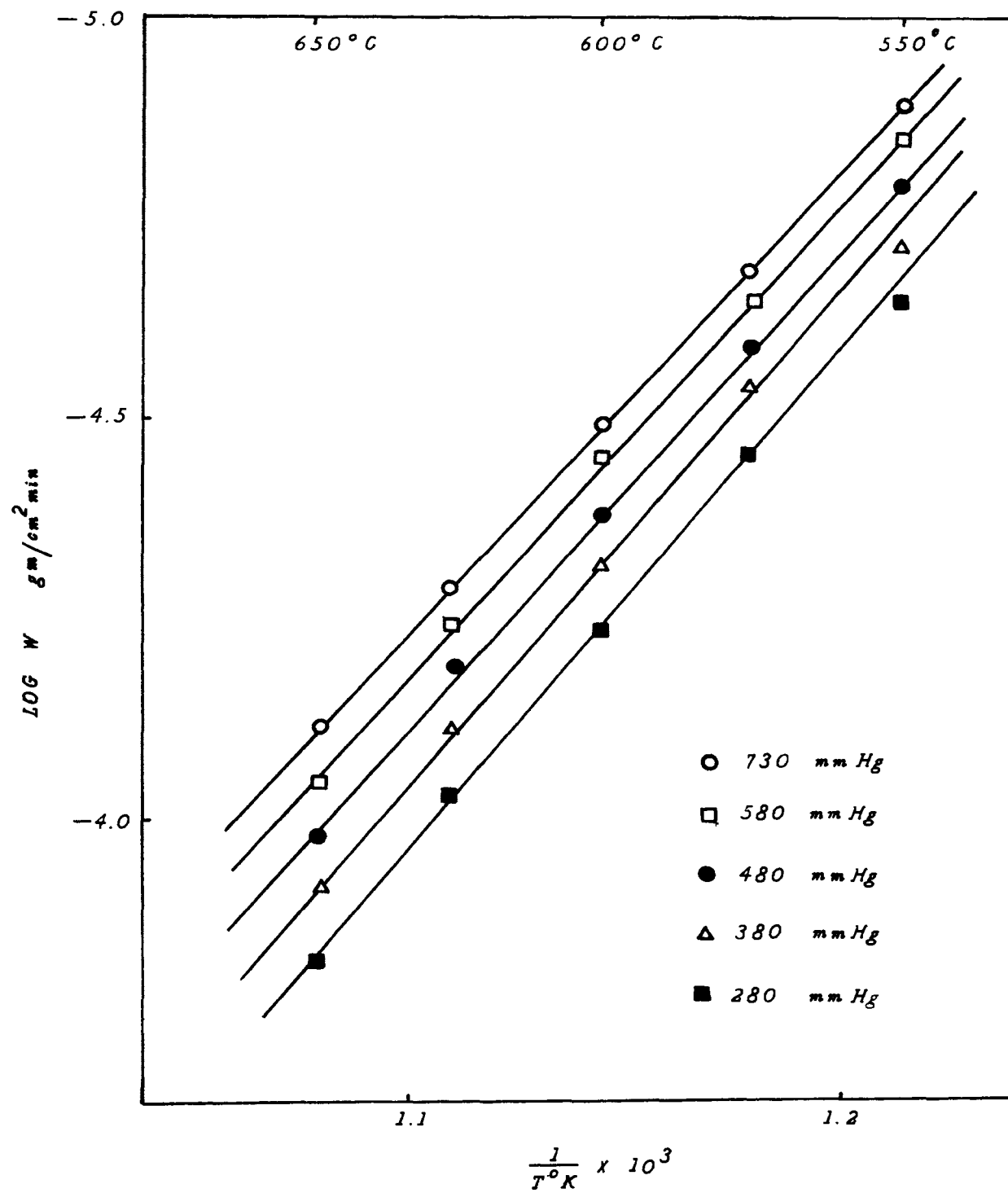
EVAPORATION OF BRASS I IN ARGON

Fig. 4
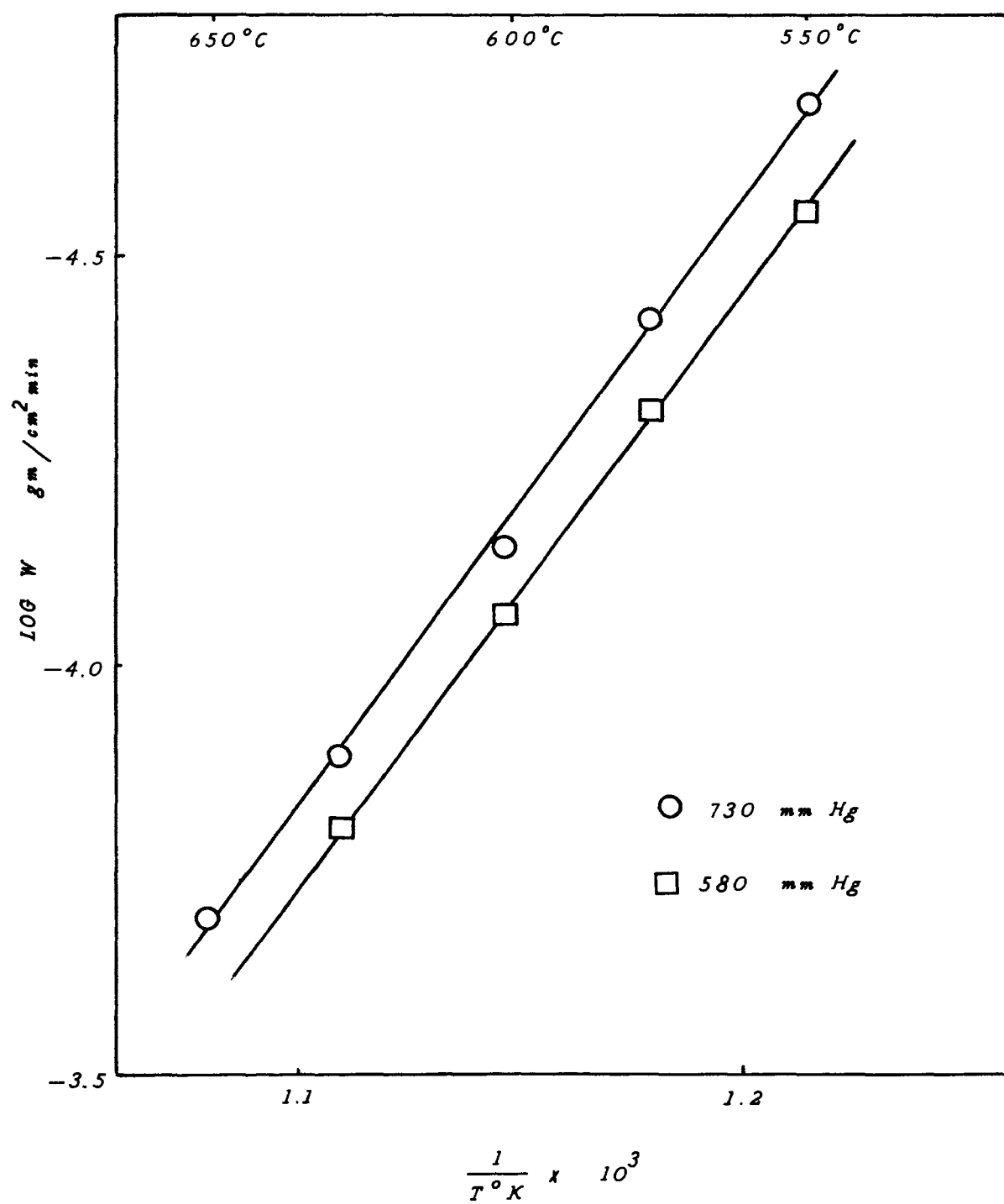
EVAPORATION OF BRASS I IN HELIUM

Fig. 5
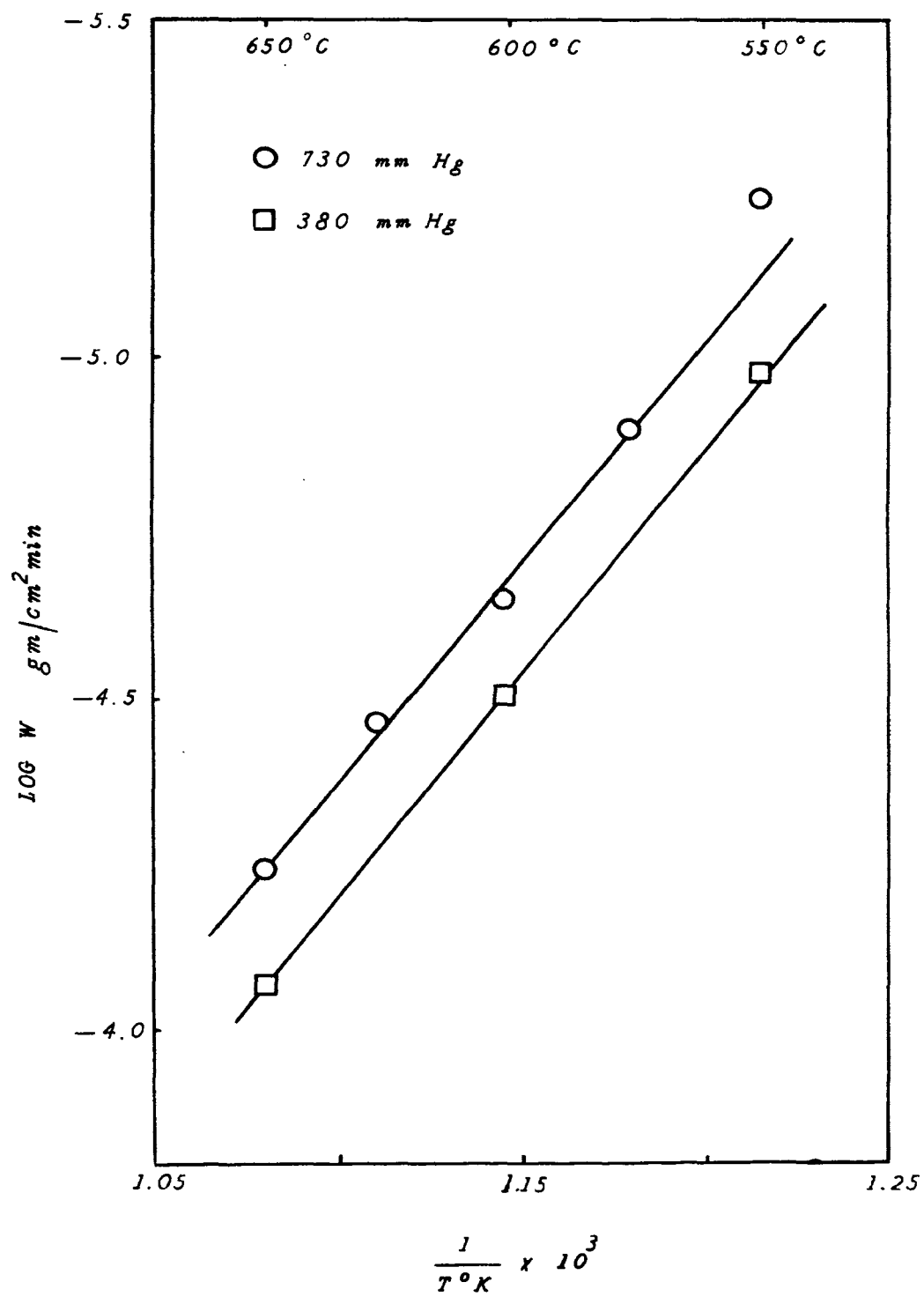
EVAPORATION OF BRASS II IN ARGON

Fig. 6
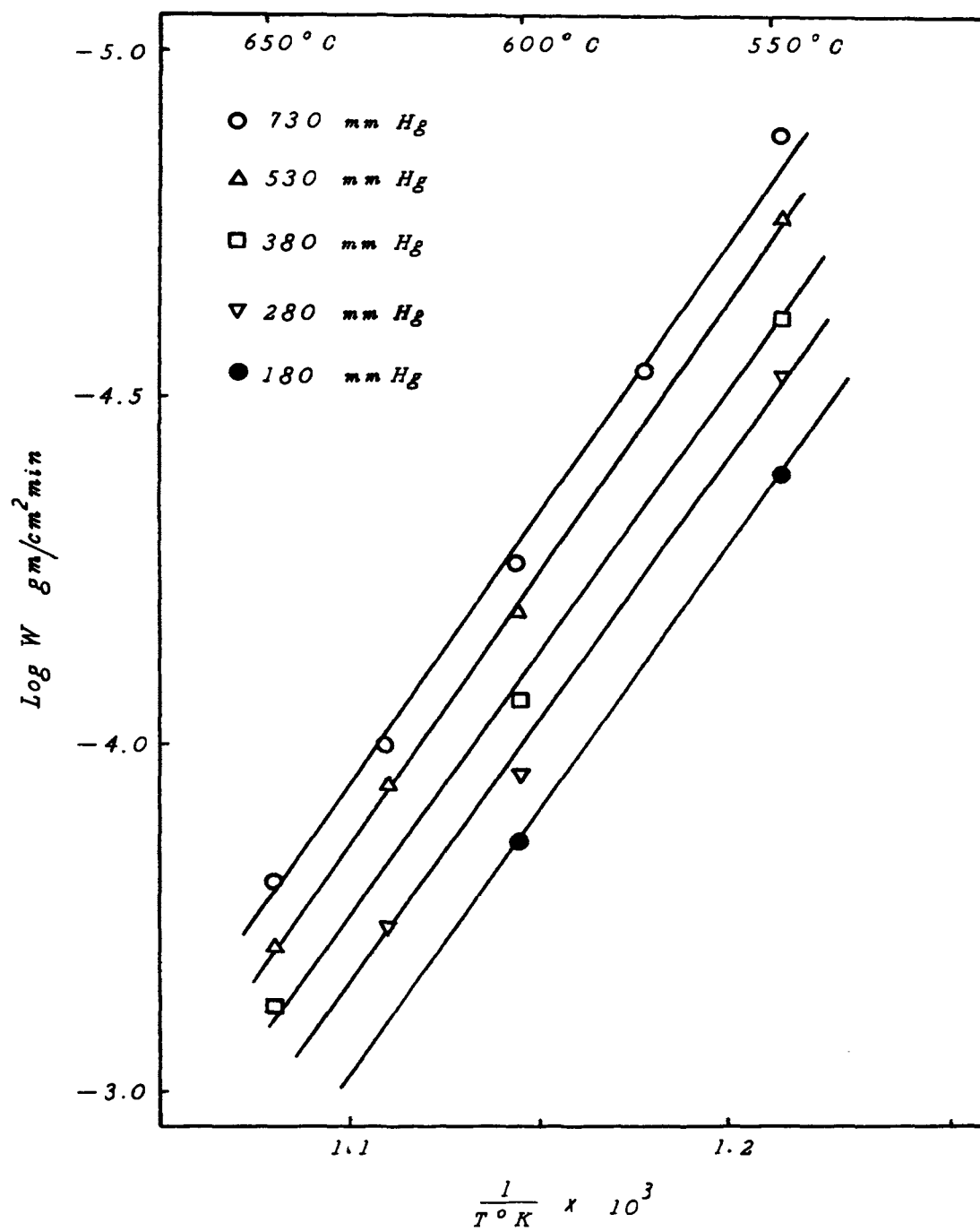
EVAPORATION OF BRASS II IN HELIUM

Fig. 7
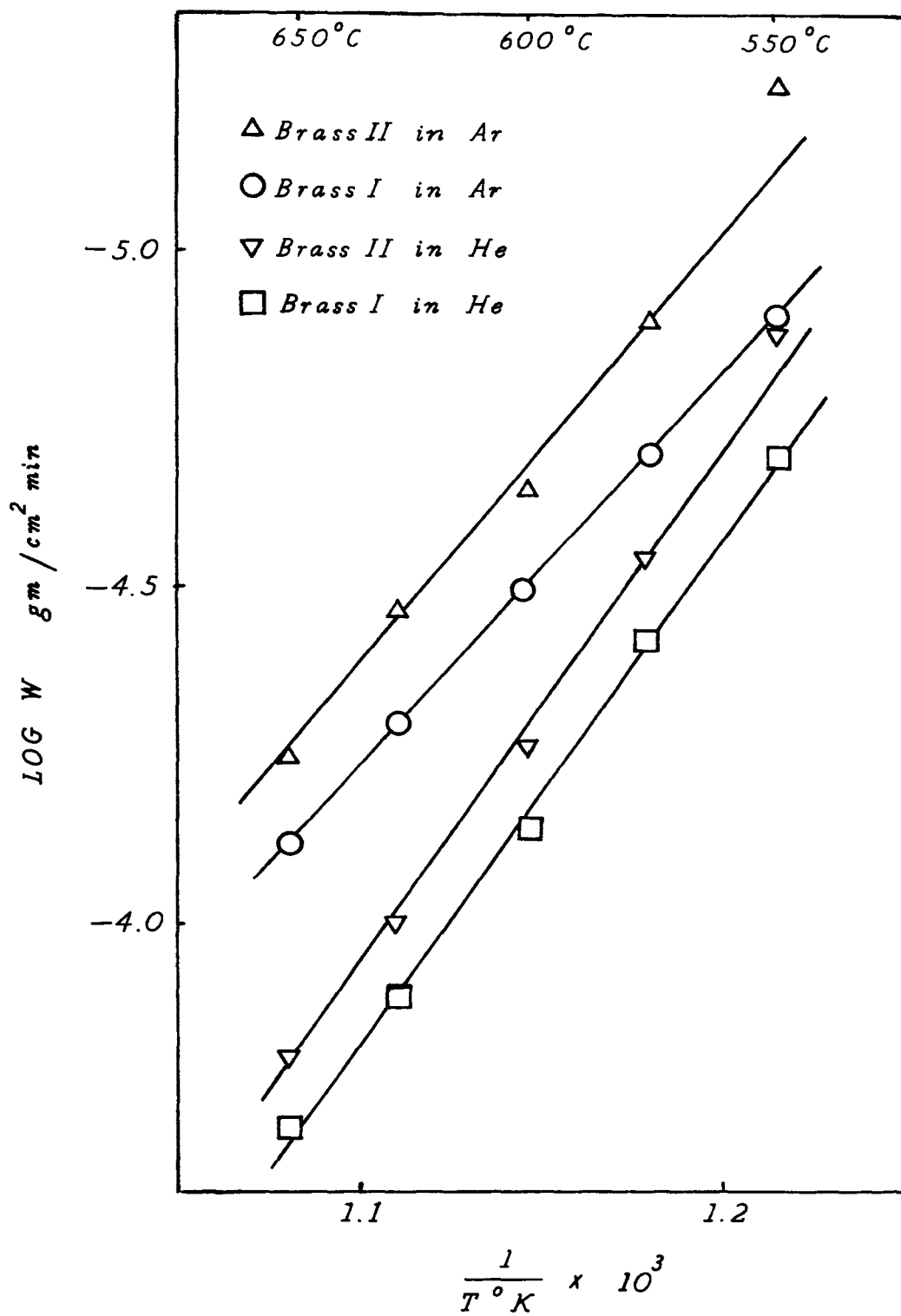
EVAPORATION OF BRASS

Fig. 8
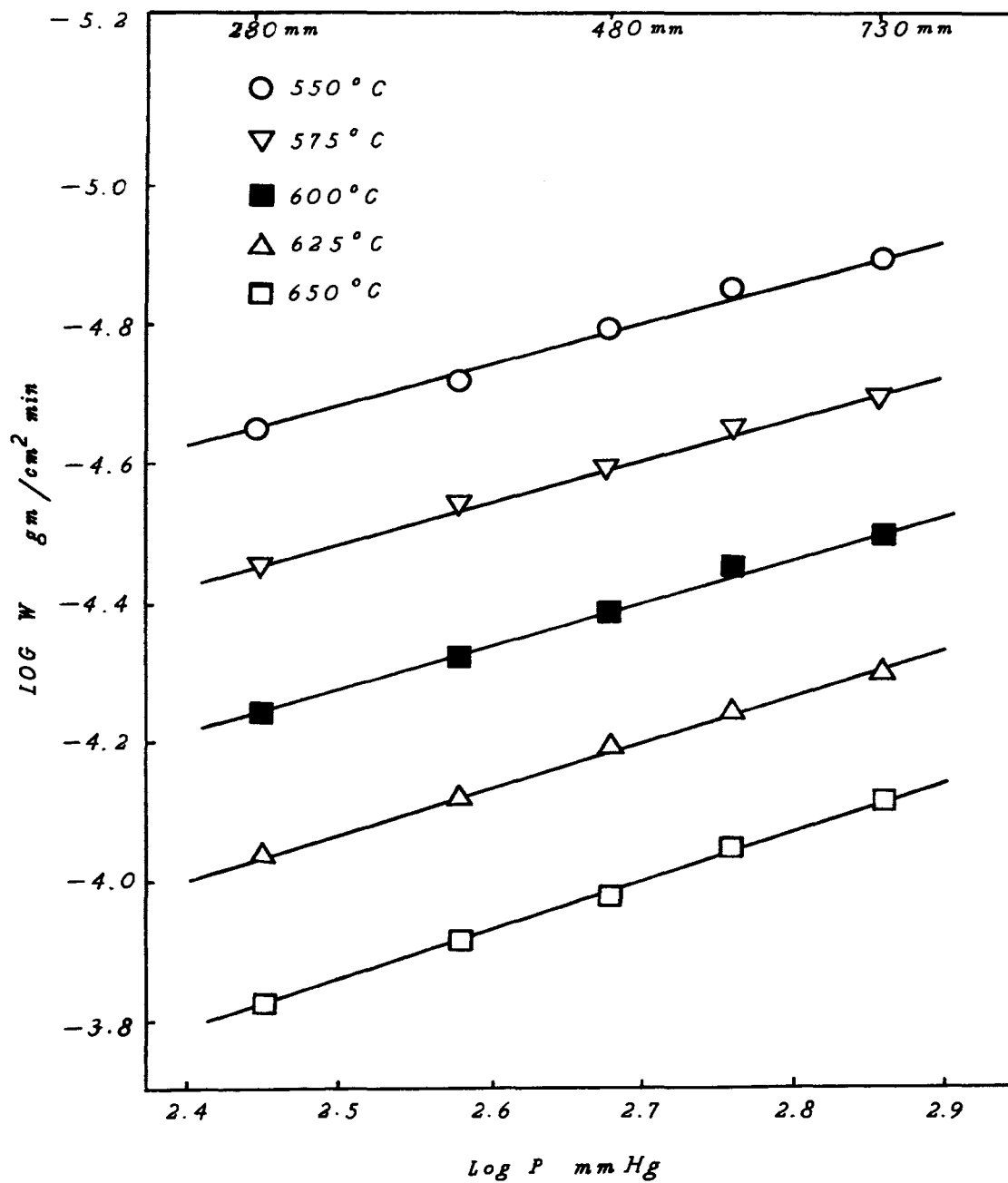
EVAPORATION OF BRASS I IN ARGON

Fig. 9
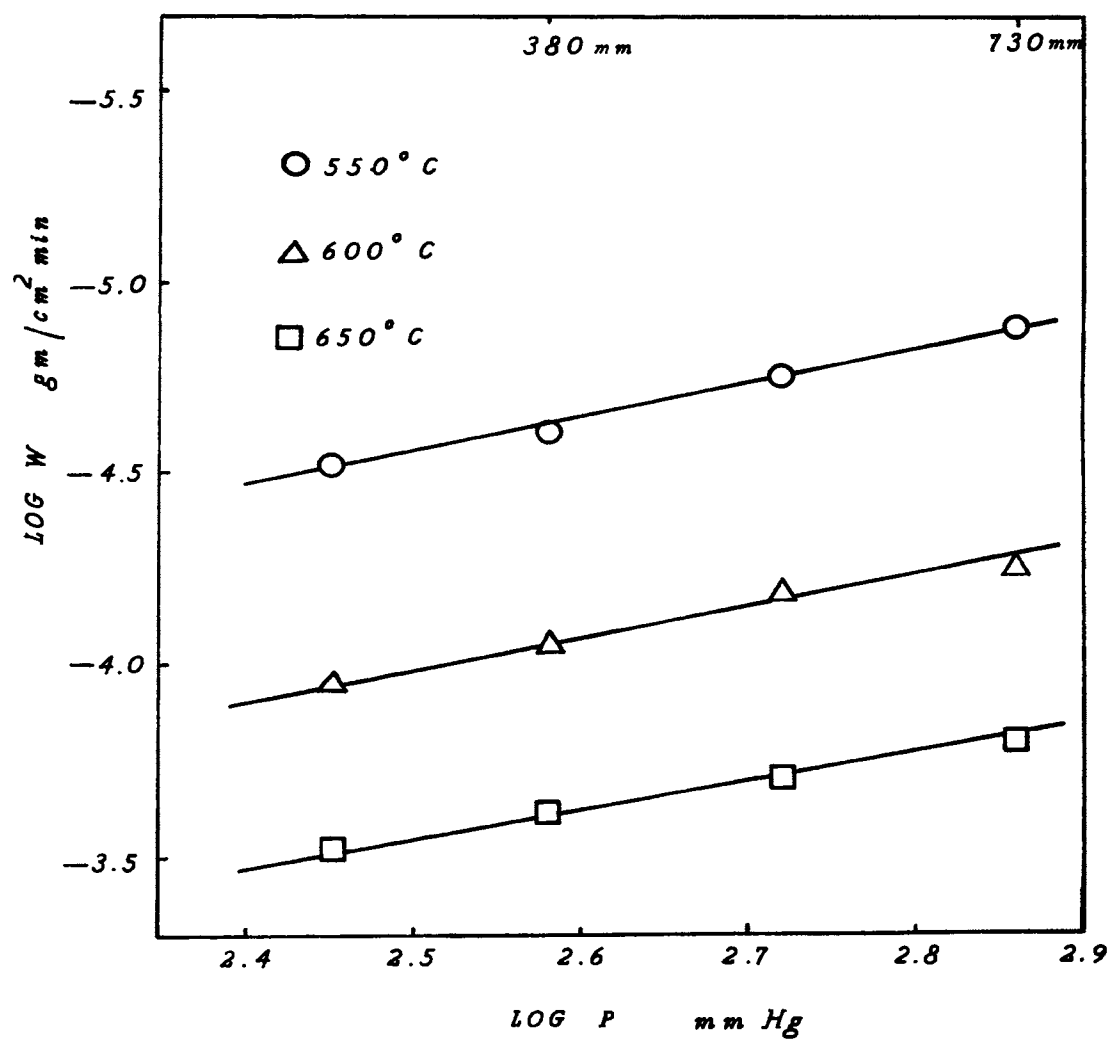
EVAPORATION OF BRASS II IN HELIUM

Fig. 10
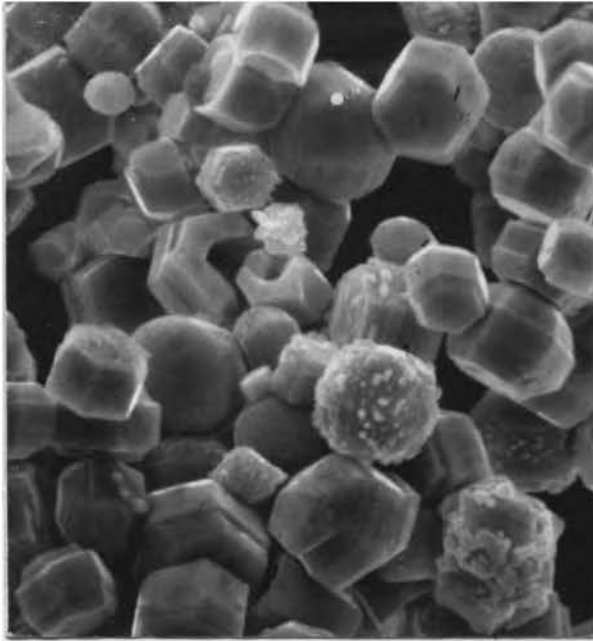
Fig. 11 Condensation of zinc

3000 x

Low Flow
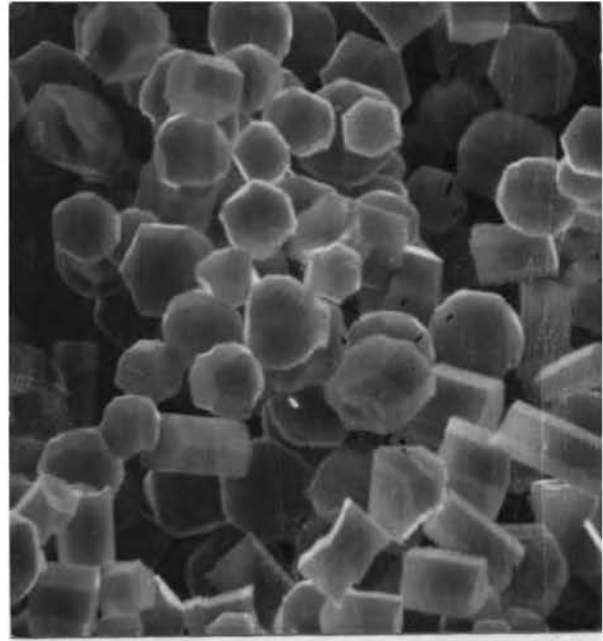
Fig. 12 Condensation of zinc

3000 x

Medium Flow
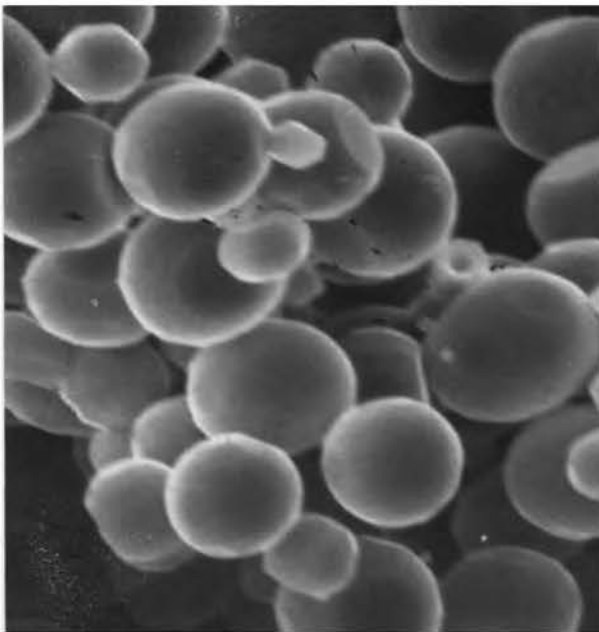
Fig. 13 Condensation of zinc

3000 x

Continued Growth
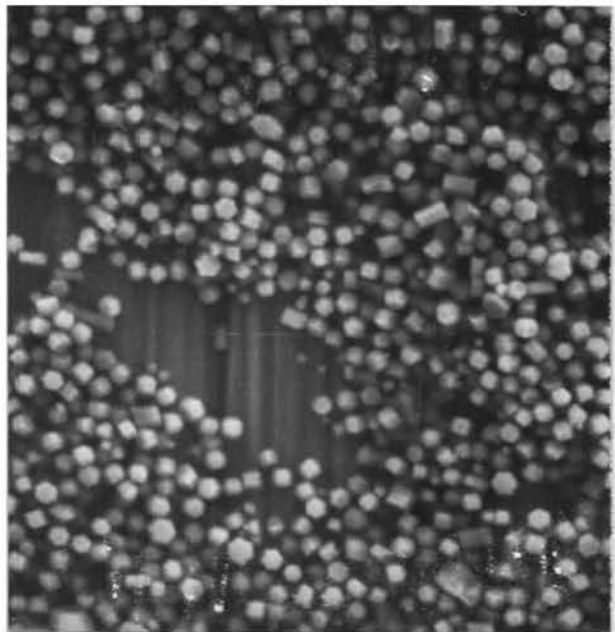
Fig. 14 Condensation of zinc

1000 x

Medium Flow, Longer Time
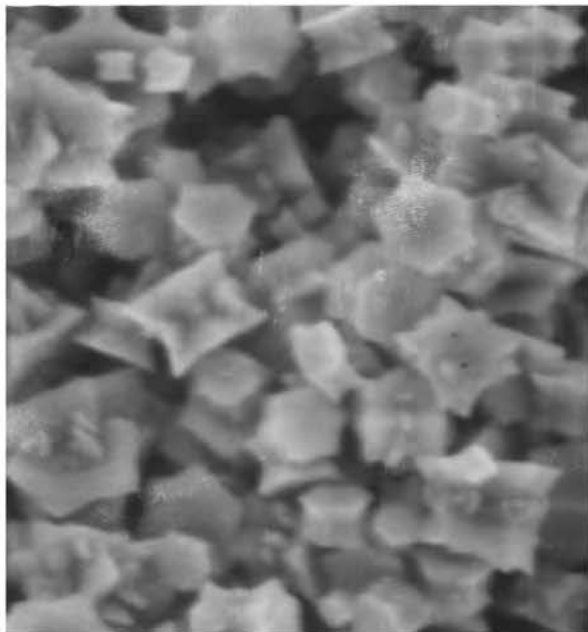
Fig. 15 Condensation of zinc
3000 x
Helium
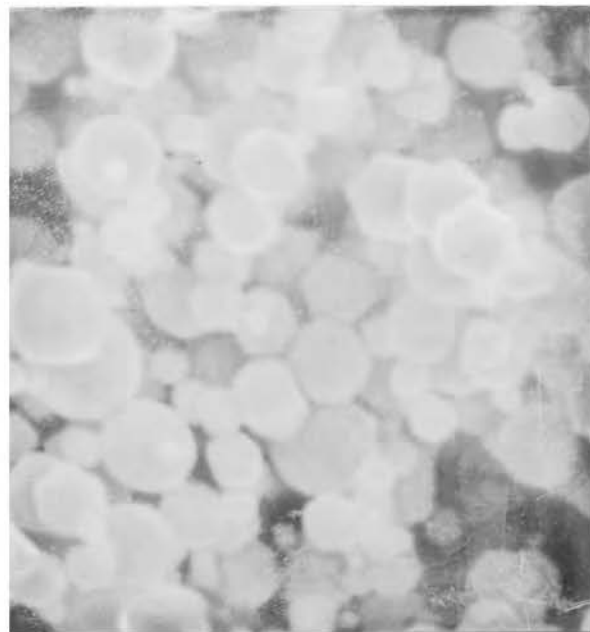
Fig. 16 Condensation of zinc
3000 x
Low Pressure
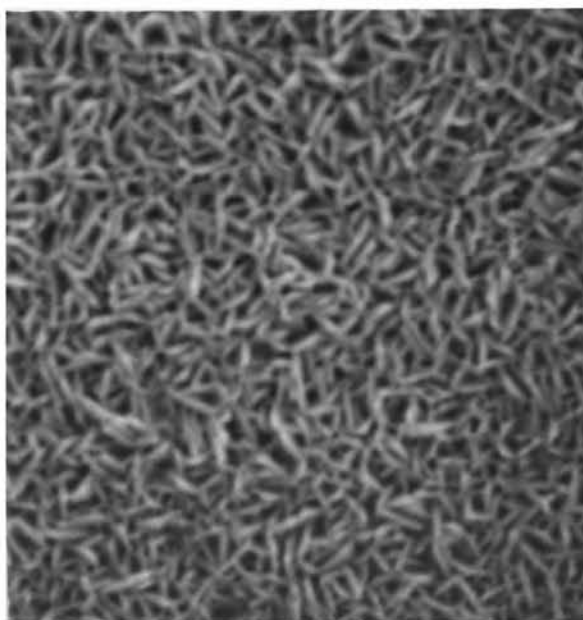
Fig. 17 Condensation of zinc
3000 x
Initial Film
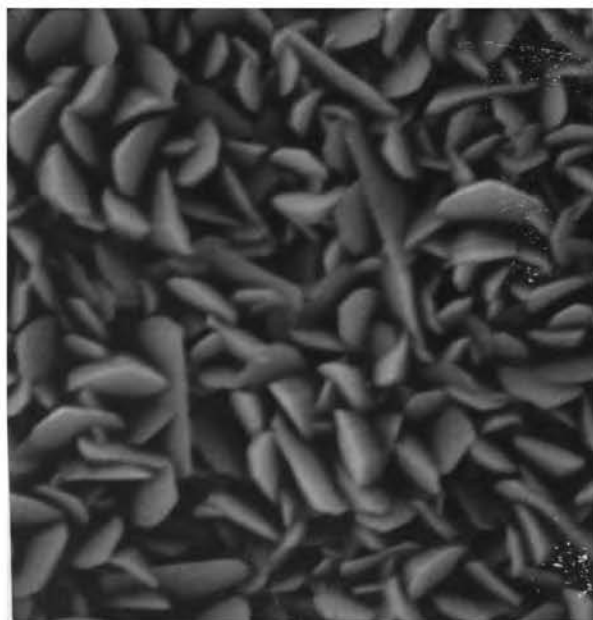
Fig. 18 Condensation of zinc
3000 x
Final Growth

carried completely away from the surface and does not re-condense on the surface. The W_{vac} values at the temperatures under consideration are plotted in fig. 2 with the experimentally determined rates for the purpose of comparison. The vapor pressure values for zinc used here for calculating W_{vac} are those reported by Barrow et. al.[7]. The evaporation rates are also plotted in fig. 3 as Log W vs. Log P where P is the pressure of residual gas.

Fig. 4, 5, 6, and 7 show the Arrhenius type plots of the sublimation rates of Brass I in argon, Brass I in helium, Brass II in argon, and Brass II in helium respectively. Fig. 8 shows the rates for all four cases at one atmosphere total pressure, for comparison. Sublimation rates of Brass I in argon and Brass II in helium are also plotted in fig. 9 and 10 respectively, as Log W vs. Log P where P is the total pressure in mm Hg. The sublimation rates of brass powders were found to be independent of the amount of brass, within the range of time for which these experiments were conducted, as long as there was sufficient amount to cover the entire cross-sectional area of the crucible.

Fig. 11 to 19 show the micrographs of zinc condensate produced under various conditions. Fig. 11 to 16 represent the condensate in the form of powder, collected from the inside bottom of the tube. These powders correspond to condensation at comperatively high total pressures. At pressures lower than 10-20 mm Hg, the metal condenses in the form of a continuous film over the surface of the vycor tube and the structure of these films is shown in figs. 17 to 19.
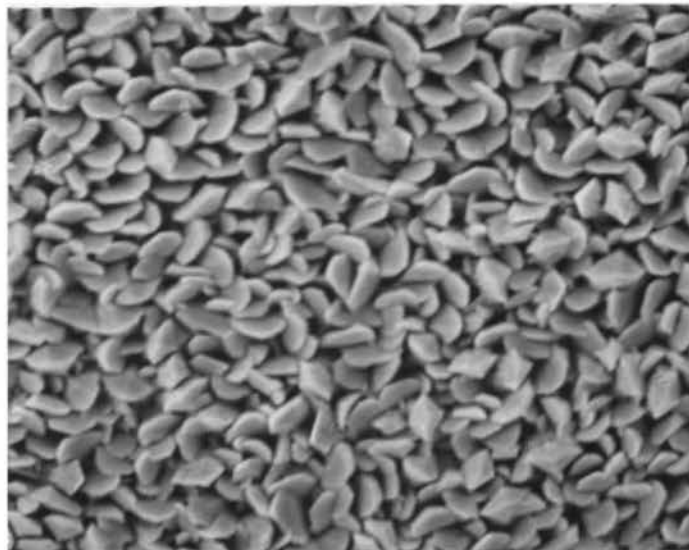
Fig. 19 Condensation of zinc

3000 x

Helium

Fig. 20 Evaporation apparatus

DISCUSSION AND CONCLUSIONS

Evaporation

Various equations have been derived for determining the rates of evaporation of liquids in inert atmospheres. For the present work, rates were calculated using the Maxwell-Stefan law of molecular diffusion[8], using a diffusion constant D calculated along the lines indicated by Gambill[9] and Wilke and Lee[10] (See Appendix A). The experimentally obtained rates of evaporation of zinc are found to be about 10 times as high as those predicted by these equations at one atmosphere. There are a number of factors which can contribute to this difference. The theoratical equations are based on the assumption that the evaporation and condensation surfaces are equal and parallel. In the present experimental arrangement, the condensation surface, though not exactly determinable, will be much larger than the evaporating surface. Also, the equations do not take into account the convection currents within the furnace tube. The difference between the observed and calculated rates decreases as the residual gas pressure decreases. This could well be expected, as decreasing the pressure also reduces the extent of the convection currents.

The average activation energy of evaporation of liquid zinc, calculated using the lines shown in fig. 2 is 29.06 K Cal/mole. The most striking features of this plot are that this energy remains practically independent of pressure and that the rates
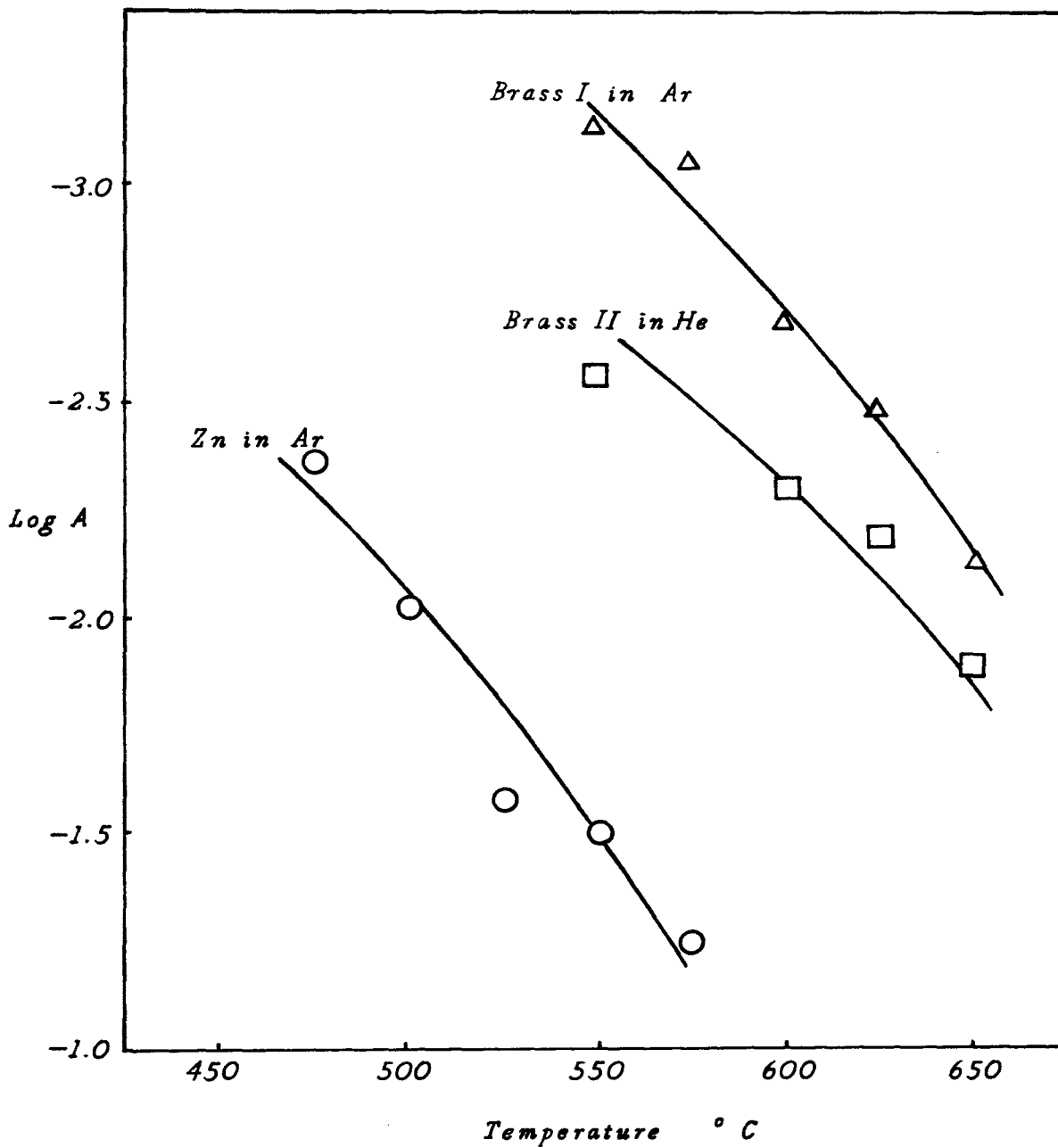
EVAPORATION OF ZINC AND BRASS

Fig. 21

approach the maximum theoratical rates, W_{vac}, in an orderly manner.
The straight line corresponding to W_{vac} gives an activation energy
of 29.8 D Cal/mole which agrees well with the observed value of
29.06 K Cal/mole. Similarly, activation energies for Brass I in
argon: 27.6 K Cal/mole, Brass I in helium: 34.28 K Cal/mole, Brass II
in argon: 31.93 K Cal/mole, and Brass II in helium: 35.16 K Cal/mole.
As shown in fig. 8, the sublimation rates of Brass I are higher
both in argon and helium than those for Brass II by a factor of 1.2
to 1.3. This may be due to slightly higher zinc content in Brass I
(30% vs. 27%). Also, diffraction pattern of Brass II shows the
presence of extra lines which may suggest the possibility of a second
phase containing lesser amount of zinc.

Examination of figs. 3, 9, and 10 would indicate that due to
the linear dependence between Log W and Log P, a relationship can
be found of the form $W=AP^B$ for the evaporation of liquid zinc or
sublimation of zinc from Brass in argon and in helium. Based on
the observed rates in the present investigation and using a linear
least squares plot, it can be shown that

$$W_{zn} = A_{zn} \, P^{-0.73} \quad \text{in argon}$$

$$W_{Brass\ I} = A_{Brass\ I} \, P^{-0.63} \quad \text{in argon}$$

$$W_{Brass\ II} = A_{Brass\ II} \, P^{-0.66} \quad \text{in helium}$$

where W is the rate of evaporation or sublimation in gm/cm^2 min., B
is a constant for a given system, B independent of pressure and
temperature, A is the temperature coefficient for a given system, and
P is the pressure of residual gas in mm Hg. The values of A
determined in the present work are plotted in fig. 21. It can be
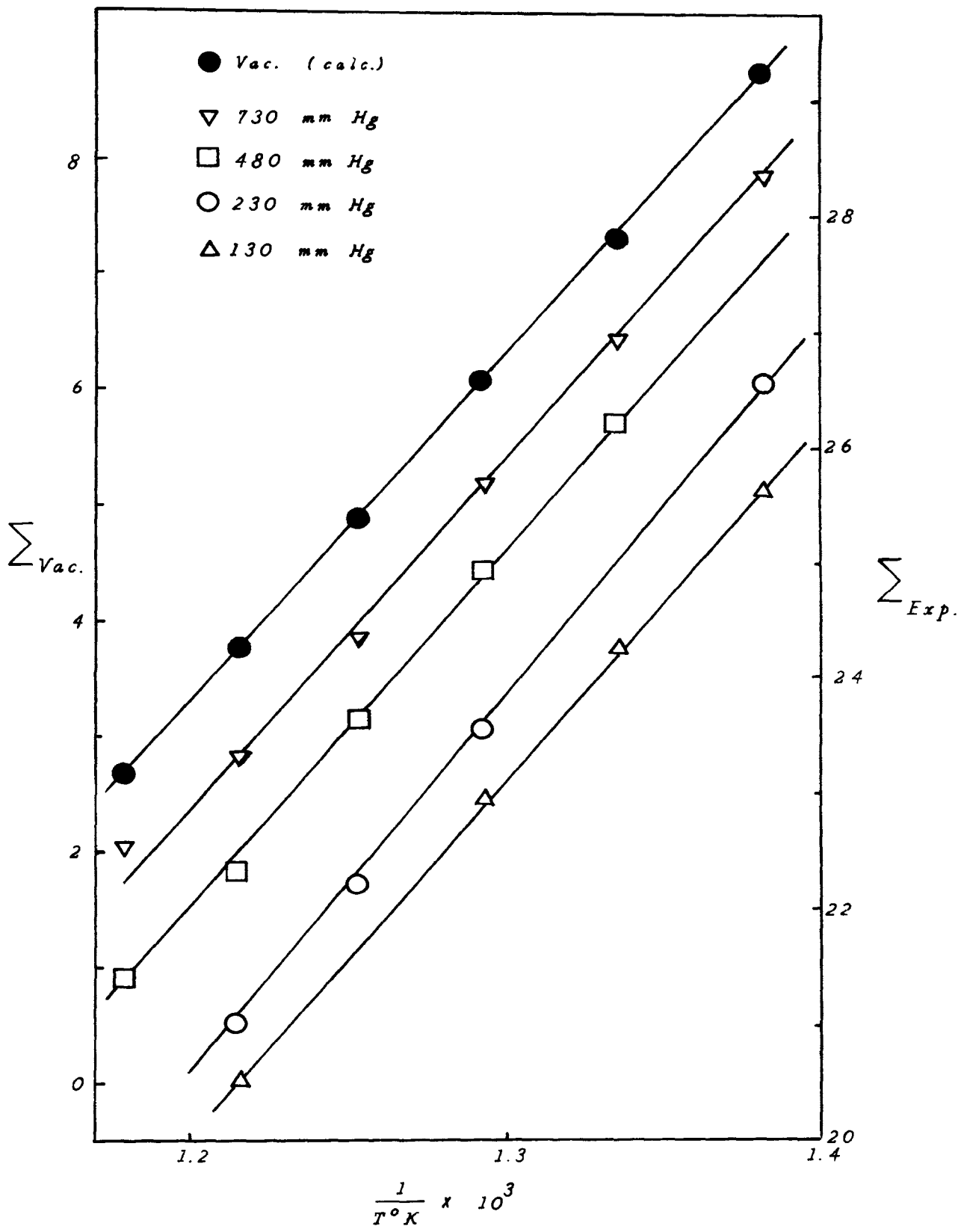
Fig.22   EVAPORATION OF ZINC

seen from this plot that the sublimation behavior of brass is similar to the evaporation of liquid zinc.

Considering the evaporation of liquid zinc once again,

$$\Delta C_p = C_{pg} - C_{pl} = \Delta a + \Delta bT$$

and

$$\Delta H^O = \int \Delta C_p dT = \Delta Ho + \Delta aT + \frac{\Delta bT^2}{2}$$

where ΔHo is an integration constant.

Combining this with the van't Hoff's equation

$$\frac{d \ln k}{dT} = \frac{\Delta H^O}{RT^2}$$

gives,

$$R \, d\ln k = \frac{\Delta Ho \, dT}{T^2} + \frac{\Delta a dT}{T} + \frac{\Delta b}{2} \, dT$$

which, when integrated gives

$$R \, \ln k = - \frac{\Delta Ho}{T} + \Delta a \ln T + \frac{\Delta b}{2} T - I$$

where I is another integration constant.

Since for evaporation of a pure metal, $R \ln k = R \ln p$ where p is the vapor pressure of volatile species,

$$-R \, \ln p + \Delta a \, \ln T + \frac{\Delta b}{2} T = \frac{\Delta Ho}{T} + I \qquad (3)$$

Now the left hand side of equation (3) is usually designated as Σ. Hence,

$$\Sigma = \frac{\Delta Ho}{T} + I$$

For zinc, $\qquad C_{pl} = 7.09 + 1.15 \times 10^{-3}T \qquad$ (Darken and Gurry[11])

and $\qquad\qquad\qquad C_{pg} = 4.96 \qquad\qquad$ (Barrow et al.[7])

Hence, $\qquad \Sigma = -R\ln p - 2.12 \, \ln T - 0.575 \times 10^{-3}T$

Using the partial pressure values of zinc given by Barrow et al.[7], Σvac. can be calculated. These values are plotted versus 1/T in fig. 22.

If it is assumed that the behavior of zinc is ideal to the extent that even in presence of an inert gas, the simple, kinetic
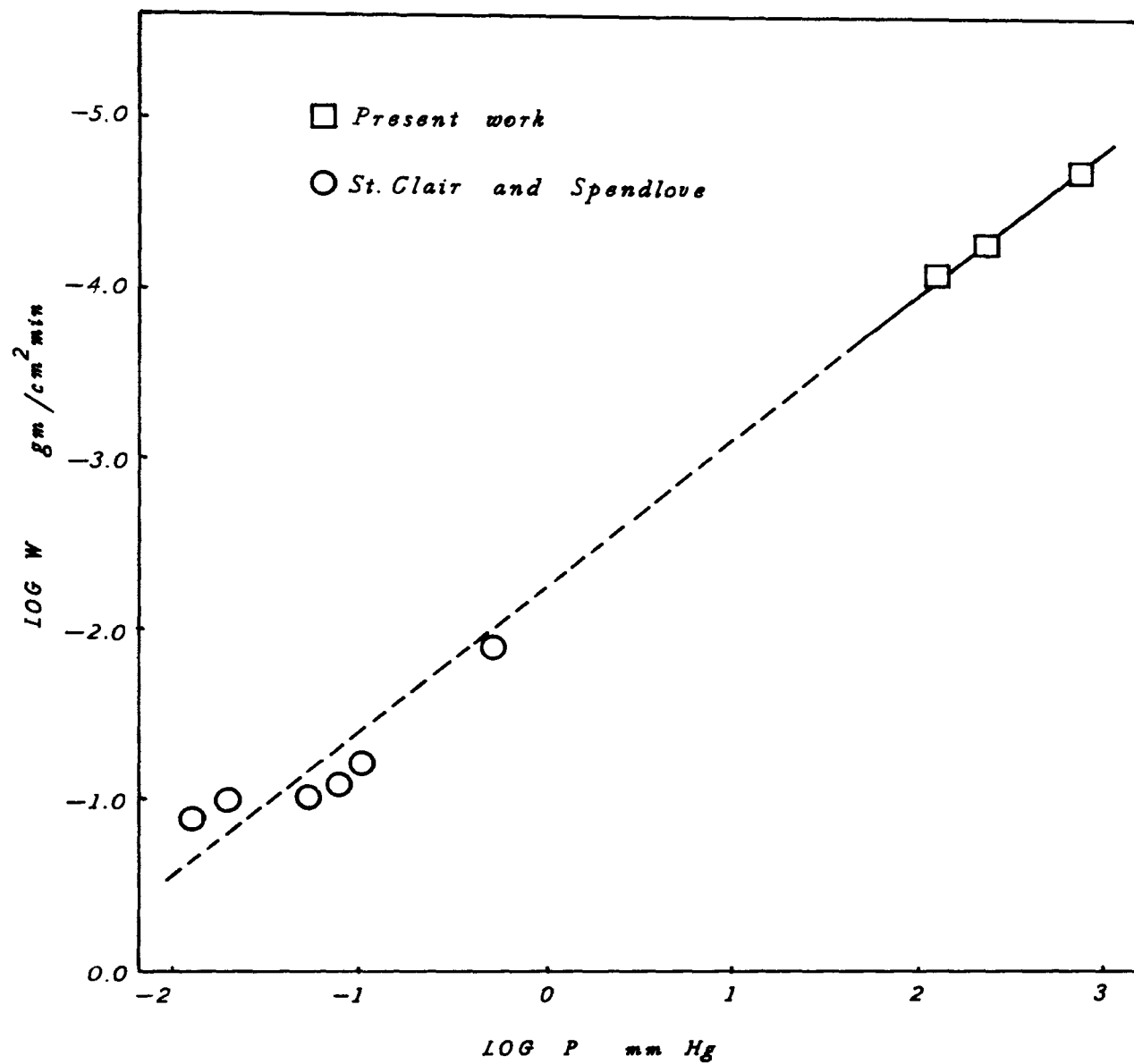
EVAPORATION OF ZINC

Fig. 23

theory equation of zinc evaporation in vacuum is still applicable; equation (2) can be used for comparison. Knowing the experimentally obtained rates of evaporation, W, the "effective vapor pressure" of zinc in argon can be calculated using equation (2) and these values of "vapor pressure" can be used to calculate Σ values at different temperatures and total pressures. This has been done to obtain Σ_{exp} values which are plotted in fig. 22 along with Σ_{vac}. The similarity between these curves in fig. 22 indicates the very nearly ideal nature of zinc evaporation as well as the applicability of kinetic theory principles to the process.

As mentioned previously, St. Clair and Spendlove[1],[2] have experimentally determined the evaporation rate of zinc at very low pressures and these experiments were conducted on a much larger scale than the present work. Their results for 450°C are plotted and compared with the observed rates in the present investigation in fig. 23. This plot indicates the strong possibility of using data obtained on a small experimental apparatus to approximate results which might be obtained in a larger, commercial scale operation.

Condensation of Zinc

From equilibrium considerations, Kaishev and Nanev [12] have shown that the structure of crystals grown from the vapor phase depends on the degree of supersaturation and that at very low supersaturation, zinc should form crystals bound by $\{0001\}$, $\{10\bar{1}0\}$, $\{10\bar{1}1\}$, $\{10\bar{1}2\}$, $\{11\bar{2}0\}$, $\{11\bar{2}1\}$, and $\{1\bar{1}22\}$. The $\{11\bar{2}0\}$, $\{11\bar{2}1\}$ and $\{11\bar{2}2\}$ faces will vanish at higher supersaturation and at still higer values for the vapor

supersaturation, the crystals will be bound by only {0001}, {10$\bar{1}$0} and {10$\bar{1}$1} faces.

In the present investigation, the degree of supersaturation is determined not by the control of temperature of the bulk vapor and of the condensation site, but by the transfer of argon gas from the hot region to the cooler region. In effect, higher gas flow should result in higher effective supersaturation. Fig. 11 shows particles formed at a comparatively low flow rate ($\simeq$ 10 cc/min.) of argon and collected nearer to the source of vapor. As can be seen, the majority of the crystals show only {0001} and {10$\bar{1}$0} faces. At still higher rates ($\simeq$ 30 cc/min.) a distinct absence of faces other than {0001} and {10$\bar{1}$0} is noticed as in fig. 12. However, if these crystals are allowed to grow further by some means, as when they are kept suspended in vapor phase due to eddy currents in the tube, they result in almost spherical particles as shown in fig. 13. These particles still display the {0001} face in certain cases. If this further growth can be prevented, a large amount of zinc powder can be produced, consisting of crystals bound by only {0001} and {10$\bar{1}$0} faces. Fig. 14 shows the result of just such an attempt, keeping a very high gas flow ($\simeq$ 40 cc/min.) over the liquid metal bath.

Fig. 15 shows particles formed using helium as the residual gas. The reasons for the formation of apparent twin crystals in the atmosphere of helium can not be explained at the present time.

Fig. 16 shows crystals formed at a lower argon residual gas pressure (200 mm Hg). These crystals are similar to those formed at one atmosphere pressure.

At still lower pressures, below 10-20 mm Hg, the deposit

morphology changes drastically. Distinct particles do not form any more and, instead, a continuous film is formed over the entire surface. The structure of this film is independent of the material on which the deposition takes place. Fig. 17 shows an early stage of formation of such a film. The deposit obtained after an increase in deposition time (approximately 15 min.) is shown in fig. 18. The formation of this film appears to be independent of the nature of residual gas, as seen in fig. 19 which shows the deposit formed in an atmosphere of helium.

BIBLIOGRAPHY

1. St. Clair, H.W., and Spendlove, M.J., U.S. Bureau of Mines Report of Investigation 4710, June 1950.

2. St. Clair, H.W. and Spendlove, M.J., J. of Metals, 191, 1951, 1192.

3. Wu, C.S., The inert gas effect on the rate of evaporation of Zinc and Cadmium, Thesis, Univ. of Missouri-Rolla, 1968 .

4. Wada, N., Jap. J. of App. Phy., 6, 1967, 553.

5. Butler, J.F., J. of Vac. Sci. and Tech., I, 1970, S52.

6. Glasstone, S., Textbood of Physical Chemistry, D.Van Nostrand Co., Inc., 1946, 276.

7. Barrow, R.F., Dodsworth, P.G., Downie, A.R., Jeffries, A.N.S., Pugh, A.C.P., Smith F.J., and, Swinstead, J.M., Trans. Faraday Soc., 51, 1955, 1354.

8. Lorian, M.G., Mass Transfer, Prentice-Hall, Inc., Englewood Cliffs, N.J., 1958, 168.

9. Gambill, W.R., Chem. Eng. 65, 1938, 125.

10. Wilke, C.R. and Lee, C.Y., Ind. Eng. Chem., 47, 1955, 1253.

11. Darken, L.S. and Gurry, R.W., Physical Chemistry of Metals, McGraw Hill Book Co., Inc., 1953, 228.

12. Kaishev, R and Nanev, C., Growth of Crystal, vol. 7, Consultants Bureau, Washington, 1969, 19.

APPENDIX A

Theoretical Rate Calculations

Gilliland's equation for diffusion of gaseous metal 1 in inert gas 2 is given as:

$$D_{1,2} = \frac{0.0047 \ T^{3/2} \left(\frac{M_1 + M_2}{M_1 \ M_2} \right)^{1/2}}{P (V_1^{1/3} + V_2^{1/3})^2}$$

To calculate the diffusivity at 723 K (450 C) and one atmosphere pressure, the following values were used:

T = 723°K

M_1 = Molecular weight of zinc = 65.38 gm.

M_2 = Molecular weight of argon = 39.94 gm.

P = Total pressure = 1 atm.

V_1 Molal volume of metal zinc at its normal boiling point

= 20.4 cm³/gm. mole

V_2 = Molal volume of argon at its normal boiling point

= 24.3 cm³/gm. mole

Using these values,

$$D_{Zn,Ar} = 0.58 \ cm^2/sec. \text{ at } 723°K \text{ and } 1 \text{ atm.}$$

Maxwell-Stefan equation for rate of evaporation is:

$$W = \frac{60(P)(M_{zn})(D)(P_{zn_{723°k}} - P_{zn_{298°k}})}{(\lambda)(R)(T)(P_{Ar_{298°k}} - P_{Ar_{723°k}})} \ \text{In} \ \frac{P_{av_{298°k}}}{P_{Ar_{723°k}}}$$

Where M_{zn} = Molecular weight of zinc = 65.38 gm.

D   = The diffusivity of zinc in argon at 723°K, 1 atm.

= 0.58 cm²/sec

$P_{zn_{723°k}}$ = The partial pressure of zinc at evaporation surface.

= 0.37 mm Hg

$P_{zn_{298^\circ k}}$ = The partial pressure of zinc at condensing surface.

$\simeq 0$

$P_{Ar_{298^\circ k}}$ = The partial pressure of argon at condensing surface.

= 730 mm Hg

$P_{Ar_{723^\circ k}}$ = The partial pressure of argon at evaporating surface.

= 730 - 0.37 = 729.63 mm Hg

λ = The distance between evaporating and condensing surface.

$\simeq$ 8 cm.

R - Gas constant - 82.0 cm^3-atm/$^\circ$k-mole

T = 723°K

Using these values,

W_{zn} = 2.62 x 10^{-6} gm/cm^2 min. at 723°K, 1 atm.

APPENDIX B

Rates of Evaporation

Evaporation of zinc in Argon

Temp$^\circ$C	W gm/cm^2 min			
	730 mm Hg	480 mm Hg	230 mm Hg	130 mm Hg
450	2.14×10^{-5}	2.88×10^{-5}	5.37×10^{-5}	8.32×10^{-5}
475	4.26×10^{-5}	6.31×10^{-5}		1.66×10^{-4}
500	7.85×10^{-5}	1.12×10^{-4}	2.24×10^{-4}	3.02×10^{-4}
525	1.44×10^{-4}	2.09×10^{-4}	4.07×10^{-4}	
550	2.30×10^{-4}	3.89×10^{-4}	7.58×10^{-4}	9.33×10^{-4}
575	3.98×10^{-4}	6.02×10^{-4}		1.58×10^{-3}

Evaporation of Brass II in Argon

Temp° C	W gm/cm min	
	730 mm Hg	380 mm Hg
550	5.78×10^{-6}	1.04×10^{-5}
575	1.28×10^{-5}	
600	2.30×10^{-5}	3.17×10^{-5}
625	3.46×10^{-5}	
650	5.78×10^{-5}	8.37×10^{-5}

Evaporation of Brass I in Helium

Temp° C	W gm/cm min	
	730 mm Hg	580 mm Hg
550	2.04×10^{-5}	2.63×10^{-5}
575	3.80×10^{-5}	4.89×10^{-5}
600	7.24×10^{-5}	8.70×10^{-5}
625	1.28×10^{-4}	1.58×10^{-4}
650	2.04×10^{-4}	

Evaporation of Brass II in Helium

Temp $^\circ$C	W gm/cm^2 min				
	730 mmHg	530 mmHg	380 mmHg	280 mmHg	180 mmHg
550	1.32×10^{-5}	1.73×10^{-5}	2.42×10^{-5}	2.95×10^{-5}	4.07×10^{-5}
575	2.88×10^{-5}				
600	5.49×10^{-5}	6.45×10^{-5}	8.7×10^{-5}	1.09×10^{-4}	1.38×10^{-4}
625	1.00×10^{-4}	1.14×10^{-4}		1.82×10^{-4}	
650	1.58×10^{-4}	1.69×10^{-4}	2.39×10^{-4}	3.02×10^{-4}	

Evaporation of Brass I in Argon

Temp °C	W gm/cm² min				
	730 mm Hg	580 mm Hg	480 mm Hg	380 mm Hg	280 mm Hg
550	1.27×10^{-5}	1.39×10^{-5}	1.59×10^{-5}	1.90×10^{-5}	2.24×10^{-5}
575	2.03×10^{-5}	2.23×10^{-5}	2.54×10^{-5}	2.89×10^{-5}	3.50×10^{-5}
600	3.18×10^{-5}	3.49×10^{-5}	4.14×10^{-5}	4.78×10^{-5}	5.75×10^{-5}
625	5.10×10^{-5}	5.70×10^{-5}	6.36×10^{-5}	7.64×10^{-5}	9.24×10^{-5}
650	7.63×10^{-5}	8.91×10^{-5}	1.05×10^{-4}	1.21×10^{-5}	1.48×10^{-4}

APPENDIX C

EVAPORATION OF ZINC ALLOYS

Some experiments were carried out to study the effect of
alloying additions on the rate of evaporation of zinc. Within the
experimental error, additions of 1% Pb, 1% Su, and 5% Sn did not
appear to alter the rates of evaporation.

It has been previously known that the addition of aluminum
tends to increase the evaporation rates of zinc, particularly
at temperatures in the range of 900°C. During the present work, rates
were determined with 1% aluminum in the liquid zinc bath. In all
cases, the rates were found to be lower than those corresponding to
pure zinc, possible due to the formation of a continuous film of
aluminum oxide on the surface.

Temp $^{\circ}$C	W gm/cm^{2}min.		
	1% Pb	1% Sn	5% Sn
500	1.05×10^{-4}	9.77×10^{-5}	8.31×10^{-5}
550	3.05×10^{-4}	3.31×10^{-4}	2.39×10^{-4}
600	6.76×10^{-4}	6.02×10^{-4}	4.89×10^{-4}

VITA

Shailesh B. Vora was born on January 17, 1945 in Gota, India. He attended G. T. High School in Bombay and later joined Elphinstone College, Bombay for the degree of Intermediate Science. He received B.Tech. in Metallurgical Engineering from the Indian Institute of Technology, Bombay in 1967.

He enrolled in the University of Missouri-Rolla for an M.S. in Metallurgical Engineering in September, 1968.